

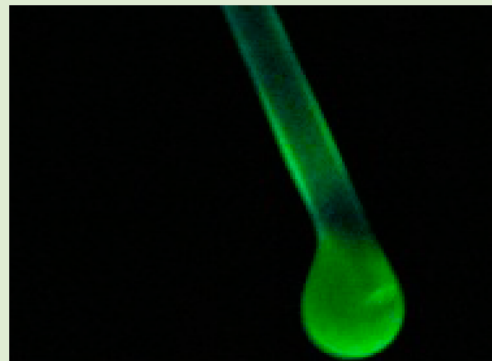
## Liquid Quantum Dots Constructed by Host–Guest Interaction

Ting Liu, Fangdan Shi, Imene Boussouar, Juan Zhou, Demei Tian, and Haibing Li\*

Key Laboratory of Pesticide and Chemical Biology (CCNU), Ministry of Education, College of Chemistry, Central China Normal University, Wuhan, 430079, People's Republic of China

## Supporting Information

**ABSTRACT:** It is a challenging task to construct nonionic liquid quantum dots (QDs) with highly optical performance. To address the problem, we make a new strategy to construct liquid QDs via host–guest interaction between  $\beta$ -cyclodextrin and adamantane. Macroscopic fluidity and optical performance of liquid QDs can be controlled by the length of polyethylene glycol. The supramolecular compounds can make use of its excellent inclusion capacities to fasten flexible organic long-chain compounds on the surface of QDs to become nonionic. Compared with the ionic liquid QDs, nonionic liquid QDs based on supramolecular self-assembly offered a strong, fast host–guest interaction, avoiding multistep reactions that would be more favorable for maintaining the fluorescent property of QDs.



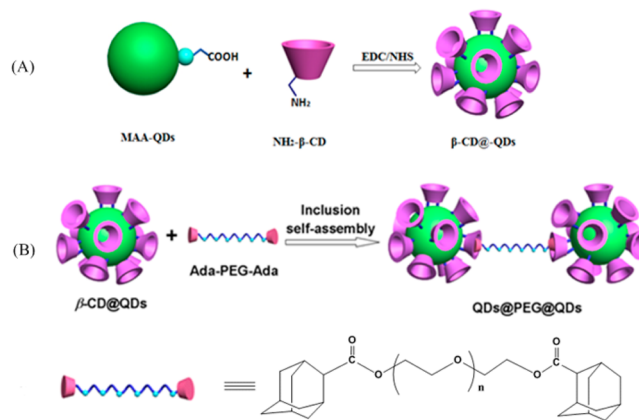
Liquid quantum dots (QDs), prepared by grafting flexible organic shells or ionic liquids on the surface of QDs, endowed QDs with fluidic behavior at low or room temperature, which has great potential application in fluorescent sensor, heat-transfer fluids,<sup>1a</sup> microfluidic devices, and so on.<sup>2</sup> Therefore, according to the different surface grafting methods, liquid QDs can be divided into ionic and nonionic liquid.<sup>3</sup> Ionic liquid QDs are used for modifying QDs through electrostatic interaction, such as ion exchanging or acid–base neutralizing reactions.<sup>4</sup> However, in the preparative experiment, the organic ligand exchanging or multistep reactions, which may influence the performance of QDs, cannot be avoided.<sup>5</sup>

Host–guest interactions have been widely used in molecule assembly,<sup>6</sup> nanoparticle assembly,<sup>7</sup> and the construction of functional materials.<sup>8</sup> For instance, it is well-known that  $\beta$ -cyclodextrin ( $\beta$ -CD) has a strong interaction to adamantane (Ada).<sup>9</sup> The excellent inclusion capacity can be used for fastening flexible organic long-chain compounds on the surface of QDs to get nonionic liquids. To our best knowledge, the research on nonionic liquid QDs has been rarely reported.

Herein, we report the first case of liquid QDs constructed via host–guest interaction. A facile one-step inclusion assembly strategy has been also employed to obtain high fluorescent liquid QDs with tunable fluidity as well as thermodynamic performance according to the length of polyethylene glycol (PEG) chains.

As shown in Scheme 1, based on the strong inclusion interaction between  $\beta$ -CD and Ada, the flexible PEG chains are grafted on the surface of QDs to assemble the liquid QDs. Scheme 1B shows the interaction and assembling schematic diagram of  $\text{QD@}\beta\text{-CD}$  and Ada-PEG-Ada. The QDs modified by mercaptoacetic acid (MAA-QDs) were prepared according to the previous report.<sup>10</sup> The fluorescence quantum yield<sup>11</sup> of

**Scheme 1.** (A) Synthetic Route of  $\text{QD@}\beta\text{-CD}$ ; (B) Diagram of the Interaction between  $\text{QD@}\beta\text{-CD}$  and Ada-PEG-Ada



the MAA-QDs is calculated to be 60%. Then CdTe QDs have been modified with  $\beta$ -CD in advance according to the reported process.<sup>12</sup>

Meanwhile, the fluorescence quantum yield of the  $\text{QD@}\beta\text{-CD}$  is calculated to be 49%, which is obviously lower than CdTe QDs. The reason is that after being modified with  $\beta$ -CD, the QDs have gathered together because of the intermolecular hydrogen bonding among  $\beta$ -CDs on the surface of QDs. Adamantane terminated PEG chains with different lengths have been successfully synthesized.<sup>13</sup> The fluorescence quantum yield of  $\text{QD@}\beta\text{-CD} + \text{Ada-PEG600-Ada}$  is 47%, as the  $\text{QD@}\beta\text{-CD} + \text{Ada-PEG2000-Ada}$  is 43%. What we can see is that, as the

Received: December 17, 2014

Accepted: March 12, 2015

Published: March 13, 2015

modification of QD proceeds, the fluorescence quantum yield has decreased. This phenomenon is coincident with the gradually fluorescence quenching in Figure S1B. It can be found that, with the interaction between QD@ $\beta$ -CD and the Ada-modified PEG chain, the system shows slight fluorescence reducing and blue shift. Through comparison and analysis, we can find that the fluorescence reducing phenomenon becomes more and more obvious with the increase of the length of PEG chain. This is probably caused by the aggregation of QDs because the flexible PEG chains may twine with each other. The fluorescence lifetime of the materials has been detected in Figure S2. As it can be seen, with the reduction of the fluorescence quantum yield, the fluorescence lifetime of the samples reduced after formation of the supramolecular system.

Infrared spectra of QD@ $\beta$ -CD are shown in Supporting Information (Figure S1). In contrast to the original mercaptoacetic acid (MAA) modified CdTe QDs, the characteristic absorption of  $\beta$ -CD appeared at  $1073\text{ cm}^{-1}$ , indicating that  $\beta$ -CD has been modified on the surface of QDs successfully. Figure S1C,D is the infrared spectra of liquid QDs (QD@ $\beta$ -CD + Ada-PEG-Ada). The chains of PEG characteristic peaks can be found in the spectra: C–O–C stretching vibrations at  $1105$  and  $1115\text{ cm}^{-1}$  and ester groups at  $1725\text{ cm}^{-1}$ , which could indicate that the surfaces of the QDs have been successfully modified with PEG chains. In addition, the fluorescence emission spectra show that the fluorescence intensity of QDs has reduced after being modified with  $\beta$ -CD, which is coincident with the reducing of fluorescence quantum yield and the report in the literature.<sup>14</sup> This has further supported the successful preparation of QD@ $\beta$ -CD.

Remarkably, the microscopic morphology of liquid QDs has been analyzed by transmission electron microscope (Figure 1).

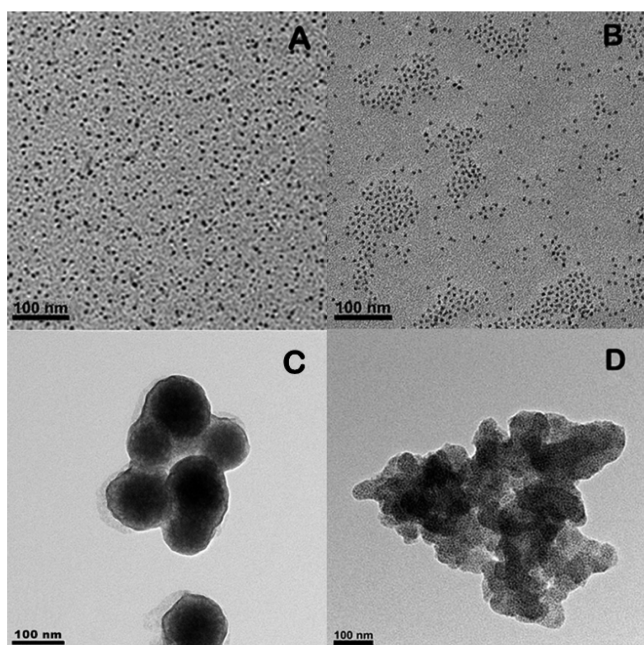


**Figure 1.** TEM photo of MAA-QDs (A) are dispersed well in water; QD@ $\beta$ -CD (B), the QDs modified by  $\beta$ -CD showed slightly gathered phenomenon; QD@ $\beta$ -CD + Ada-PEG600-Ada (C), QDs pretend obvious spherical structure because of chain wrapping; QD@ $\beta$ -CD + Ada-PEG2000-Ada (D), QDs show random aggregation due to the long flexible PEG chains. It indicates that the composited nanostructure is controlled by the length of PEG chains.

First, we can see the QDs are dispersed well in water (Figure 1A). However, QDs modified by  $\beta$ -CD display slight gathering phenomenon (Figure 1B). This may be attributed to the intermolecular hydrogen bonding among  $\beta$ -CDs on the surface of QDs in the solvent. But after adding Ada-PEG-Ada, the assembling structures of QDs have changed obviously. With the reaction between QD@ $\beta$ -CD and Ada-PEG600-Ada, QDs have wrapped up successfully to form spherical structure (Figure 1C). However, after adding the Ada-PEG2000-Ada, liquid QDs have presented to be random aggregation, which may be formed by the strong entangling interactions between the long flexible PEG chains (Figure 1D). Through the comparative analysis of microscopic morphology, it can be concluded that the length of the PEG chain decisively influences the assembling morphology of the QDs. Therefore, the possible assembling structure has been put forward. It is considered that the short PEG chain performs extension status in this new kind of liquid QD. However, when the PEG chain becomes too long, the overwhelming entanglement between flexible chains results in QDs gathering. This is coincident with the fluorescent property of liquid QDs modified by different lengths of PEG chains, which would have inspiring potential application in fluid materials with different fluorescent properties.

Here, the fluorescent thermal stability of QDs has been studied in Figure S3. The rising temperature has caused a continuous decrease in the fluorescence intensity and red shift (Figure 3SA), which illustrates the thermal instability of the QD series, including QD@ $\beta$ -CD + Ada-PEG600-Ada and QD@ $\beta$ -CD + Ada-PEG 2000-Ada. However, from the slope it can be seen the different speeds and degrees of quenching. Particularly, the QDs assembled by PEG600 and PEG2000 present a slow trend of fluorescence intensity decrease. In addition, the cycles of the fluorescent intensity have been tested in Figure S4. As expected, when the temperature is  $10\text{ }^{\circ}\text{C}$ , the different materials exhibited great intensity of fluorescence, but when the temperature rises to  $30\text{ }^{\circ}\text{C}$ , the intensity of the fluorescence decreased remarkably. When the temperature returned to  $10\text{ }^{\circ}\text{C}$ , the intensity of fluorescence recovered to some degree. Among these recycles, it can be seen that the QDs assembled by PEG600 pretended to have excellent thermo-stability, while QDs assembled by PEG2000 took second place on the stability. It can be guessed that the PEG can adjust the stability of fluorescence by extending chains and steadying the QDs in the solvent to some degree.

The thermodynamic properties of the two assembled liquid QDs are shown in Figure 2. As shown in thermogravimetric analysis (TGA), both of the two liquid QDs have a slight thermal mass loss below  $100\text{ }^{\circ}\text{C}$  at the initial stage. This is mainly caused by the evaporation of trace solvent remaining in the materials. A fraction of thermal weightlessness appears within the temperature range from  $100$  to  $300\text{ }^{\circ}\text{C}$  for the thermal decomposition of  $\beta$ -CD and the organic ligands on the surface of QDs. During the whole heating process, the two liquid QDs assembled by different lengths of PEG chains have a similar thermogravimetric curve, with the thermal mass loss rates of 62% for PEG600 + QD@ $\beta$ -CD and 64% for PEG2000 + QD@ $\beta$ -CD. The main mass loss at the temperature ranging from  $300$  to  $420\text{ }^{\circ}\text{C}$  is due to the thermal weight loss of flexible PEG chains.<sup>15</sup> The content of PEG chains coupled on the surface of QDs is calculated to be 54%, ensuring the flowing property of the materials. Further investigation based on DTG analysis demonstrates that the main thermal decomposition of the two assembled QDs have taken place at about  $400\text{ }^{\circ}\text{C}$ ,

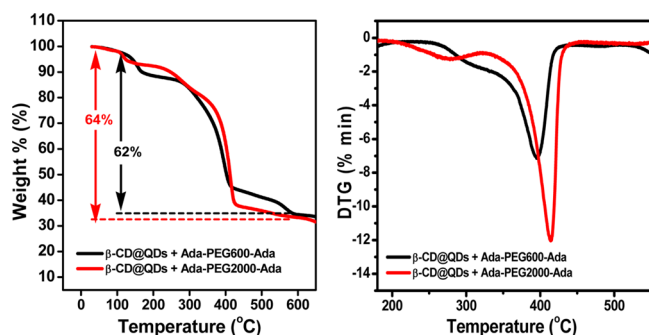


**Figure 2.** TGA (left) and micro weight curve (right) of QD@ $\beta$ -CD + Ada-PEG(600, 2000)-Ada. Fraction of thermal weightlessness appears within the temperature ranging from 100 to 300 °C for the thermal decomposition of cyclodextrin and the organic ligands on the surface of QDs; the main mass loss at the temperature ranging from 300 to 420 °C is due to the thermal decomposition of flexible PEG chains.

confirming the high thermodynamic stability of the materials. In addition, it can be found that liquid QD@ $\beta$ -CD + Ada-PEG2000-Ada has pyrolysis at about 275 °C. Consequently, liquid QD@ $\beta$ -CD + Ada-PEG600-Ada has provided better thermodynamic stability.

For further analysis of the melt-crystallization behavior during the heating process, the two liquid QDs have been characterized by differential scanning calorimetry (DSC) measurements (Figure S5). In a sharp contrast, liquid QDs assembled by PEG600 present melt crystallization behavior at lower temperature with the endothermic peak at 1.6 °C and the exothermic peak at  $-30.2$  °C, while QD@ $\beta$ -CD + Ada-PEG2000-Ada have a higher phase transition temperature with an endothermic peak at 56.9 °C and an exothermic peak at 14.5 °C. In this case, the phase-transition property of liquid QDs prepared by the proposed method can be tailored by simply changing the length of the flexible PEG chains.

Figure 3A demonstrates the macroscopic flowing properties of liquid QDs modified with PEG2000. The modified QDs are a yellow waxy solid, which has obvious great green fluorescence. With the temperature increasing, the distinct solid–liquid transition appeared. The phase inversion temperature is about

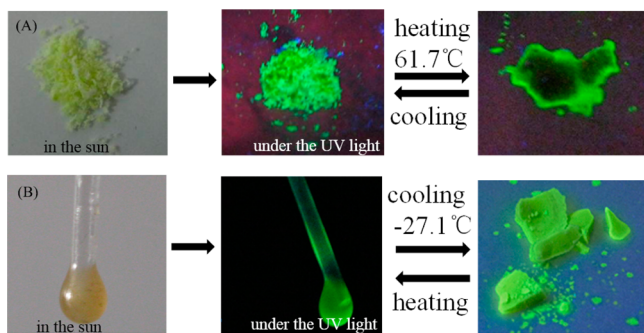


**Figure 3.** (A) Photo of the liquidity of QD@ $\beta$ -CD + Ada-PEG2000-Ada (ultraviolet excitation: 365 nm); it performs to be a faint yellow waxy solid, while it shows obvious green fluorescence under an ultraviolet lamp, and when the temperature rises up to 61.7 °C, it shows a solid–liquid transforming property obviously, while it turns back to solid when cooling down to room temperature. (B) Photo of the liquidity of QD@ $\beta$ -CD + Ada-PEG600-Ada (ultraviolet excitation: 365 nm); it performs to be obviously fluid, and when the temperature cools down to  $-27.1$  °C, it turns to solid. As a result, the temperature-sensitive fluidity can be controlled by the length of PEG chains.

61.7 °C, but the red shift of fluorescence is observed for QDs modified by PEG2000 in the experiment, so the stability of material remains to be further improved. However, QDs modified by PEG600 show a preferable flow property at room temperature (Figure 3B), when the temperature cools down to  $-27.1$  °C, they turn to solid. Notably, the material keeps fluorescent performance well. As it can be seen, the properties they have shown are coincident with DSC shown in Figure S2. As a result, we can draw the conclusion that the PEG chain can adjust the rheological temperature of the QDs material.

In conclusion, we have successfully synthesized a new kind of liquid QD assembled with PEG chains by host–guest interaction. This method is considered to be easy, convenient, fast, as well as having improved the fluorescence quantum yield. The materials are of great optical property, and they are a thermosensitive multifunction sensor as well, which not only shows that the QDs assembled by the unique host–guest interactions can be conveniently controlled with desirable properties, but can also guide us to develop more functional fluidic materials, such as smart fluidic sensors.

## ■ ASSOCIATED CONTENT

### 📄 Supporting Information

Synthesis and characterizations of all the products, including  $^1\text{H}$  NMR spectra, infrared spectra, fluorescence emission spectra, and DSC spectra. This material is available free of charge via the Internet at <http://pubs.acs.org>.

## ■ AUTHOR INFORMATION

### Corresponding Author

\*E-mail: [lhbing@mail.ccnu.edu.cn](mailto:lhbing@mail.ccnu.edu.cn).

### Notes

The authors declare no competing financial interest.

## ■ ACKNOWLEDGMENTS

This work was financially supported by the National Natural Science Foundation of China (21372092, 21102051), Natural Science Foundation of Hubei Province (2013CFA112, 2014CFB246), and self-determined research funds of CCNU from the colleges' basic research and operation of MOE (CCNU13F005, CCNU14Z010 01).

## ■ REFERENCES

- (1) (a) Warren, S. C.; Banholzer, M. J.; Slaughter, L. S.; Giannelis, E. P.; Disalvo, F. J.; Wiesner, U. B. *J. Am. Chem. Soc.* **2006**, *128*, 12074. (b) Bourlinos, A. B.; Herrera, R.; Chalkias, N.; Jiang, D. D.; Zhang, Q.; Archer, L. A.; Giannelis, E. P. *Adv. Mater.* **2005**, *17*, 234–237. (c) Li, Q.; Dong, L.; Deng, W.; Zhu, Q.; Liu, Y.; Xiong, C. X. *J. Am. Chem. Soc.* **2009**, *131*, 9148–9149.
- (2) Zhou, J.; Huang, J.; Tian, D. M.; Li, H. B. *Chem. Commun.* **2012**, *48*, 3596–3598.
- (3) Rodriguez, R.; Herrera, R.; Archer, L. A.; Giannelis, E. P. *Adv. Mater.* **2008**, *20*, 4353–4358.
- (4) Biswas, K.; Rao, C. N. R. *Chem.—Eur. J.* **2007**, *13*, 6123–6129.
- (5) Kim, S.; Bawendi, M. G. *J. Am. Chem. Soc.* **2003**, *125*, 14652–14653.
- (6) Stepanow, S.; Lingenfelder, M.; Dmitriev, A.; Spillmann, H.; Delvigne, E.; Li, N.; Deng, X. B.; Cai, C. Z.; Barth, J. V.; Kern, K. *Nat. Mater.* **2004**, *3*, 229–233.
- (7) Zhao, Y.; Thorkelsson, K.; Mastroianni, A. J.; Schilling, T.; Luther, J. M.; Rancatore, B. *J. Nat. Mater.* **2009**, *8*, 979–985.
- (8) Ikkala, O.; Brinke, G. *Science* **2002**, *295*, 2407–2409.
- (9) Chan, S. C.; Kuo, S. W.; Chang, F. C. *Macromolecules* **2005**, *38*, 3099–3107.

- (10) Dorokhin, D.; Hsu, S. H.; Tomczak, N.; Reinhoudt, D. N.; Huskens, J.; Velders, A. H.; Vancso, G. J. *ACS Nano* **2009**, *4*, 137–142.
- (11) Markus, G.; Monika, S.; Vladimir, L.; Nikolai, G.; Alexander, E.; Ute, R. G. *Anal. Chem.* **2009**, *81*, 6285–6294.
- (12) Desiraju, G. R. *Angew. Chem.* **1995**, *34*, 2311–2327.
- (13) Liu, S.; Weaver, J. V. M.; Save, M.; Armes, S. P. *Langmuir* **2002**, *18*, 8350–8357.
- (14) Algarra, M.; Campos, B. B.; Aguiar, F. R.; Rodriguez-Borges, J. E. *Mater. Sci. Eng.* **2012**, *32*, 799–803.
- (15) Gaponik, N.; Talapin, D. V.; Rogach, A. L.; Hoppe, K.; Shevchenko, E. V.; Kornowski, A.; Eychmüller, A.; Weller, H. *J. Phys. Chem. B* **2002**, *106*, 7177–7185.